Stable Parameter Identification Evaluation of Volatility

N. Rückert, R. S. Anderssen, B. Hofmann

Preprint 2012-3

Preprintreihe der Fakultät für Mathematik
ISSN 1614-8835

Stable Parameter Identification Evaluation of Volatility

N. Rückert*, R. S. Anderssen†, B. Hofmann*

Abstract

Using the dual Black-Scholes partial differential equation, Dupire [6] derived an explicit formula, involving the ratio of partial derivatives of the evolving fair value of a European call option (ECO), for recovering information about its variable volatility. Because the prices, as a function of maturity and strike, are only available as discrete noisy observations, the evaluation of Dupire's formula reduces to being an ill-posed numerical differentiation problem, complicated by the need to take the ratio of derivatives. In order to illustrate the nature of ill-posedness, a simple finite difference scheme is first used to approximate the partial derivatives. A new method is then proposed which reformulates the determination of the volatility, from the partial differential equation defining the fair value of the ECO, as a parameter identification activity. By using the weak formulation of this equation, the problem is localized to a subregion on which the volatility surface can be approximated by a constant or a constant multiplied by some known shape function which models the local shape of the volatility function. The essential regularization is achieved through the localization, the choice of the analytic weight function, and the application of integration-by-parts to the weak formulation to transfer the differentiation of the discrete data to the differentiation of the analytic weight function.

Keywords. Parameter identification, Volatility surfaces, Dupire's equation, Finite difference, Localization approach

1 Introduction

In financial markets, a major activity is the buying and selling of European call options (ECO), with agreed strike price $K > 0$ and maturity date $T > 0$, for some financial

*Department of Mathematics, Chemnitz University of Technology, 09107 Chemnitz, Germany. Email: nadja.rueckert@mathematik.tu-chemnitz.de, hofmannb@mathematik.tu-chemnitz.de.

†CSIRO Mathematical and Information Sciences, PO Box 664, Canberra, ACT 2601, Australia. Email: Bob.Anderssen@csiro.au

asset S with price $S(t)$ at time t. Decision-making is based on solving the appropriate parabolic partial differential equation (PPDE) which predicts the likely future fair value $C(S,t,K,T)$ of an ECO for different choices of K and T. For example, if it is assumed that the evolving price $S(t)$ of the financial asset S follows the geometric Brownian motion process

$$dS(t) = S(t)\mu dt + S(t)\sigma dW(t)$$

with drift μ, volatility σ and the standard Brownian motion $W(t)$, then the PPDE for the fair value $C(S(t),t,K,T)$ at time t takes the form

$$C_t(S,t,K,T) + rSC_S(S,t,K,T) + \frac{1}{2}\sigma^2 S^2 C_{SS}(S,t,K,T) - rC(S,t,K,T) = 0, \qquad (1)$$

for $(S,t) \in (0,\infty) \times [0,T]$ with constant short-term interest rate r and final payoff condition

$$C(S,T,K,T) = \max(S-K,0), \quad S \in (0,\infty). \qquad (2)$$

Further details can be found, for example, in [16] and [20]. However, assuming that r and $S(t)$ are known, this PPDE can only be solved once an estimate for the volatility σ has been determined. Consequently, for the ECO situation, the basic parameter identification problem (PIP) reduces to recovering estimates of the volatility σ from previously observed ECO prices $C^*(K_j,T_i)$, for different K_j and T_i values.
The drawback with the utilization of equations (1) and (2) to solve the PIP is the assumption that the volatility σ is constant. This assumption contradicts market observations that market prices of ECO never coincide with a constant volatility. To fit the theoretical option prices to the observed option prices at the market, the volatility is a function of asset price S and time t (the smile effect [9, 19]). In [7], using the dual Black-Scholes equation, Dupire derived the following alternative expression for the fair price $C(S,t,K,T)$, which is frequently called Dupire equation,

$$C_T(S,t,K,T) = \frac{1}{2}\sigma^2(K,T)K^2 C_{KK}(S,t,K,T) - rKC_K(S,t,K,T) \qquad (3)$$

for $(K,T) \in (0,\infty) \times (t,\bar{T}]$ in combination with the initial condition

$$C(S,t,K,t) = \max(S-K,0), \qquad K \in (0,\infty).$$

Here, $\bar{T}$ is the maximal maturity for which option prices are available. Consequently, the ECO PIP reduces to the determination of the volatility function $\sigma^2(K,T)$ from the

parabolic differential equation (3). For fixed time t^* and fixed asset price $S^* = S(t^*) > 0$, the observed prices of the ECO $C^*(K,T) := C(S^*, t^*, K, T)$, are given on $\Omega^* \subseteq \mathbb{R}_+ \times (t, \bar{T}]$, where it is assumed that $C^*(K,T) \in \mathcal{C}^{2,1}(\Omega^*)$. From this perspective, Dupire's equation can be rearranged to yield the following relationship [18]

$$\sigma^2(K,T) = \frac{C^*_T(K,T) + r\,K\,C^*_K(K,T)}{\frac{1}{2}\,K^2\,C^*_{KK}(K,T)}\,, \qquad (K,T) \in \Omega^*\,, \tag{4}$$

for the volatility function $\sigma(K,T)$.
It is evident that the evaluation of this formula, because of its complexity, represents a challenging task. In addition, market option data are only available at discrete points (K_k, T_l) for $1 \le k \le n$ and $1 \le l \le m$. Furthermore, it is well-known that numerical differentiation is a moderately ill-posed problem (see, e.g., [3, 12, 17]) which compounds the evaluation of the ratio in equation (4). For example, if the numerator changes sign, then unrealistic estimates for the volatilities will be obtained, or if the denominator has a small value, then extremely high estimates of the volatilities will result. As mentioned in [11], such difficulties are compounded when finite difference schemes are used to evaluate the partial derivatives. The need to perform numerical differentiation on the available discrete data, and the fact that the boundary conditions are unknown represent challenges for the evaluation of Dupire's formula (4). Another drawback is that the volatility surface $\sigma(K,T)$ can only be estimated in the subregion $\Omega^* \subseteq \mathbb{R}^+ \times (t, \bar{T}]$, whereas the volatilities on the whole region $\mathbb{R}^+ \times (t, \bar{T}]$ are required. These difficulties and the importance of estimating volatilities generate a need to explore computational alternatives. Here, following an ansatz proposed for the transmissivity estimation problem, originally in [5], we examine the use of the weak formulation of Dupire's PPDE (3) to construct alternative algorithms for the ECO PIP; in particular, a parameter identification localization (PILO) procedure. The paper [5] appealed to the fact that in transmissivity applications there is often a natural zonation structure in the geology. This point has subsequently been pursued by a number of authors including [1, 4, 10]. In our finance context, zonation of this nature does not arise. However, the volatility surface tends to change only slowly so that a piecewise constant approximation is not inappropriate.

The paper has been organized in the following manner. Notation, preliminaries and synthetic option prices are discussed in section 2. The evaluation of Dupire's formula (4) with simple finite difference schemes is examined in section 3. Because of the poor approximation of partial derivatives by finite difference schemes, as the numerical experiments of section 3 show, there is a need to consider the dual Black-Scholes equation (3) from a parameter identification perspective instead of computing the volatility surface $\sigma(K,T)$ by Dupire's formula (4). In section 4, by applying the weak formulation strategy of Chow and Anderssen [5] to equation (3), the identification of $\sigma(K,T)$ is reduced to computing constant estimates of $\sigma^2(K,T)$ on appropriately small subregions in Ω^*. The advantage of this approach is that the numerical differentiation of the available discrete data $C^*(K_k, T_l)$, $i \le k \le n$, $1 \le l \le m$, is replaced by an analytic differentiation of an appropriately chosen

analytic weight function. The numerical performance of this methodology is examined in detail in section 5. The results are summarized in section 6.
In the sequel, $\sigma^2(K,T)$ will be referred to as the volatility surface, and $\sigma_e^2(K,T)$ its computed estimate using synthetic option prices.

2 Notation, Preliminaries and Synthetic Option Prices

2.1 Synthetic Data

In the current numerical study, it is assumed, following [9], that the volatility surface $\sigma^2(K,T)$ has a separable decomposition into a price-dependent factor $\sigma_1^2(Ke^{-rT})$ and a time-dependent factor $\sigma_2^2(T)$

$$\sigma^2(K,T) = \sigma_1^2(Ke^{-rT})\,\sigma_2^2(T). \tag{5}$$

As in [9], under assumption (5), the transformations $Y = Ke^{-rT}$, $A(Y) = \frac{1}{2}\sigma_1^2(Y) = \frac{1}{20}\left[1 - \frac{1}{2}\exp\left(-4\ln^2(Y)\right)\,\sin\left(2\pi Y\right)\right]$ and $B(T) = \sigma_2^2(T) = 1 + \frac{3}{5}\sin(2\pi T)$ are used to generate synthetic option prices. Applying these transformations to Dupire's equation (3), the transformed Dupire equation becomes

$$\begin{aligned} U_\tau(Y,\tau) &= A(Y)Y^2U_{YY}(Y,\tau), && (Y,\tau) \in (0,\infty)\times(0,1], \\ U(Y,0) &= \max(S(0)-Y,0), && Y \in (0,\infty), \end{aligned}$$

where $U(Y,\tau) := C(K,T)$, $\tau(T) := \int_0^T B(t)dt$ and $\int_0^{\bar{T}} B(t)dt = 1$. In solving these equations to determine the synthetic option prices, additional boundary conditions are required, such as $U(0,\tau) = S(0)$ and $U_Y(\bar{Y},\tau) = 0$ where the initial price of the underlying asset is $S(0)$ at time $t = 0$, and the value of $\bar{Y}$ is sufficiently large.
The synthetic option prices were generated for the region $\Omega = \{(K,T) : 0 \le K \le \bar{K}, 0 \le T \le \bar{T}\}$ as explained in section 2.2 step 1. Because option prices in financial markets are non-exact, perturbed option prices were generated and examined. In the numerical investigations below, $S(0) = 1$, $r = 0.1$, $\bar{T} = 1$ and $\bar{K} = 3S(0) = 3$. For this synthetic data, "at-the-money" options corresponds to $K = 1$.

2.2 Template Structure

Computationally, the evaluation of the Dupire formula (4) and of the new parameter identification formula, defined in section 4, reduces to calculating various expressions on a template (rectangular grid) of discrete points. The former involves the evaluation of various numerical difference differentiators, while the latter involves the evaluation of appropriate quadrature formulas. The templates on which the corresponding calculations are performed are defined as follows:

1. On Ω, let G denote a fixed fine grid

$$G(n,m) = \{[K_k, T_l] : [K_0 = 0, K_1, \ldots, K_n = \bar{K}][T_0 = 0, T_1, \ldots, T_m = \bar{T}]\}$$

with grid points $[K_k, T_l]$ and $\Delta K = K_{k+1} - K_k = \frac{\bar{K}}{n}$, $k = 0, 1, \ldots, n-1$ and $\Delta T = T_{l+1} - T_l = \frac{\bar{T}}{m}$, $l = 0, 1, \ldots, m-1$. For the numerical studies reported in this paper, m and n are chosen as 2^{12}.
The synthetic option prices are generated on the template $G(n,m)$ as discussed in section 2.1.
To obtain the perturbed option prices, a matrix $\epsilon \in \mathbb{R}^{m \times n}$ of normally distributed entries $\epsilon_{kl} \sim N(0, v^2)$, $k = 1, \ldots, m$ and $l = 1, \ldots, n$ was generated with the variance v^2 determined from $E||\epsilon||_2^2 = mnv^2 \approx \delta^2$ for a chosen noise level δ. The perturbed grid data are generated as $C^\delta(K_k, T_l) = C(K_k, T_l) + \epsilon_{kl}$.

2. A representative point (K^*, T^*) is chosen in G.

3. A rectangular region $\Omega_0 = [K_0^0, K_{n_1}] \times [T_0^0, T_{n_2}] \subseteq \Omega$ is chosen with (K^*, T^*) at its center. Using grid points of $G(n,m)$, we discretize Ω_0 by

$$\begin{aligned} G_0(n_1, n_2) = \{[K_k^0, T_l^0] : [K_0 \le K_0^0, K_1^0, \ldots, K^* = K^0_{\frac{n_1}{2}}, \ldots, K_{n_1}^0 = K_{n_1} \le \bar{K}] \\ [T_0 \le T_0^0, T_1^0, \ldots, T^* = T^0_{\frac{n_2}{2}}, \ldots, T_{n_2}^0 = T_{n_2} \le \bar{T}]\} \end{aligned}$$

a set of symmetrically placed and evenly located grid points $[K_k^0, T_l^0]$ with $\Delta K^0 = K_{k+1}^0 - K_k^0$, $k = 0, 1, \ldots, n_1 - 1$ and $\Delta T^0 = T_{l+1}^0 - T_l^0$, $l = 0, 1, \ldots, n_2 - 1$. The values of the indices n_1 and n_2 control the size of Ω_0 or the fineness of the discretization performed by $G_0(n_1, n_2)$. For our numerical evaluation of Dupire's formula (4) with the finite difference scheme and the application of the PILO, we use the following specifications:

(a) **Finite Difference Scheme**

$$\begin{aligned} n_1 &= 2^p, & n_2 &= 2^q, \quad p, q = 2, 3, \ldots, 11, \\ \Delta K^0 &= \frac{K_{n_1}}{n_1} = \frac{\bar{K}}{n_1}, & \Delta T^0 &= \frac{T_{n_2}}{n_2} = \frac{\bar{T}}{n_2}. \end{aligned}$$

Consequently, through various choices of p and q, a variety of coarse and fine evenly-spaced subgrids can be chosen from G.

(b) **Parameter Identification Localization**
The region Ω_0 is chosen so that $\Omega_0 \subset \Omega$.

$$n_1 = 2^p - 2, \qquad n_2 = 2^q - 2, \qquad p, q = 2, 3, \ldots, 11,$$
$$\Delta K^0 = \Delta K = \frac{\bar{K}}{n}, \qquad \Delta T^0 = \Delta T = \frac{\bar{T}}{m}.$$

Figure 1 illustrates the template structure. The fixed fine grid $G(n, m)$ is represented by black and the varying grid $G_0(n_1, n_2)$ by blue crosses.

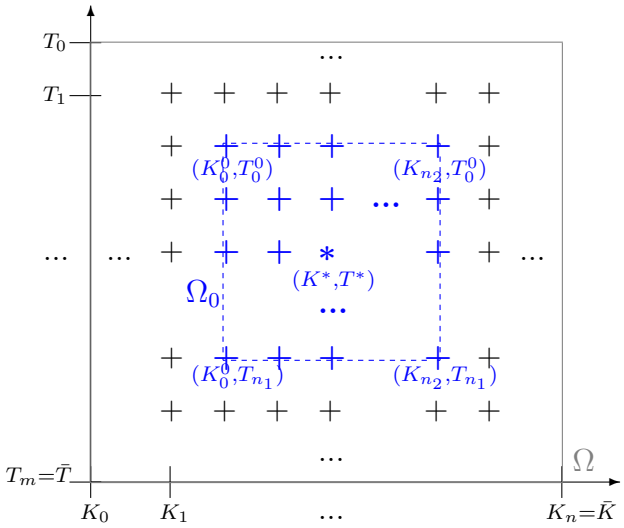

Figure 1: Template structure

2.3 Relative Error

The relative error of the computed volatility estimate in the region Ω_0, which is centered at (K^*, T^*), is evaluated as

$$R_{\Omega_0}(K, T) = \frac{||\sigma_e^2(K, T) - \sigma^2(K, T)||_F}{||\sigma^2(K, T)||_F}$$

with σ_e and σ denoting the estimated and exact values of the volatility, and

$$||\theta(K, T)||_F = \sqrt{\frac{1}{n_1 n_2} \sum_{k=1}^{n_1} \sum_{l=1}^{n_2} \left(\theta(K_k^0, T_l^0)\right)^2}$$

will be used below to asses numerical performance. Whereas the relative error at a specific point (K^*, T^*) is estimated as

$$R(K^*, T^*) = \frac{|\sigma_e^2(K^*, T^*) - \sigma^2(K^*, T^*)|}{\sigma^2(K^*, T^*)}.$$

3 Finite Difference Evaluation of Dupire's Formula

In financial mathematical deliberations, finite difference schemes are used to evaluate Dupire's formula (4) (e.g. in [11]). The utility of this approach is now explored.
We use the templates defined in section 2.2. On various grids $G_0(n_1, n_2)$, each of the partial derivatives $\partial/\partial K$ and $\partial/\partial T$ was evaluated using the corresponding equally weighted five-point-stencil (see [2]). For the second partial derivative $\partial^2/\partial K^2$ another equally weighted five-point-stencil in one dimension

$$C_{KK}(K_k^0, T_l^0) = \frac{-C(K_{k-2}^0, T_l^0) + 16C(K_{k-1}^0, T_l^0) - 30C(K_k^0, T_l^0) + 16C(K_{k+1}^0, T_l^0) - C(K_{k+2}^0, T_l^0)}{12(\Delta K^0)^2}$$

$k = 2, \ldots, n_1 - 2$ and $l = 2, \ldots, n_2 - 2$ was computed.
In order to assess the numerical performance of such finite difference algorithms for the evaluation of Dupire's formula (4), the values of n_1 and n_2 are sought which minimize, for a given choice of Ω_0 centered at $(K^*, T^*) = \left(K_{\frac{n_1}{2}}, T_{\frac{n_2}{2}}\right)$, the relative error $R_{\Omega_0}(K, T)$. It is expected that the optimum $(n_{1,opt}, n_{2,opt})$ lies between the extreme values of n_1 and n_2 because of the trade-off between error enhancement on fine discretizations and poor approximation of derivatives on coarse discretizations. The numerical experiments showed that, if Ω_0 was either too large or too small, the estimates for the volatility behaved chaotically. Consequently, the relative errors were only calculated for $\Omega_0 = [0.7, 1.5] \times [0.4, 0.8]$.

In figure 2, for the noise level $\delta = 10^{-2}$, the relative errors $R_{\Omega_0}(K, T)$ are shown for different grid sizes (n_1, n_2). For small and large values of n_1, the 5-point-stencil yields poor approximations to the volatility surface. As the figure shows clearly, the five-point-stencil approach is not as sensitive with respect to the discretization of T as to the levels of discretizations of K. This is consistent with the structure of equation (4) which only involves the first derivatives with respect to T, but first and second derivatives with respect to K. For the region $\Omega_0 = [0.7, 1.5] \times [0.4, 0.8]$, the finite difference evaluation performs well. A good insight into the nature of this approach is given in table 1.

For various choices of δ, the optimal values of n_1 and n_2 are listed which yield the smallest relative errors. This highlights the importance of the trade-off associated with choosing a medium grid size. As the noise level decreases, finer meshes can be used to improve the accuracy. This is consistent with theory because it predicts that coarser meshes are

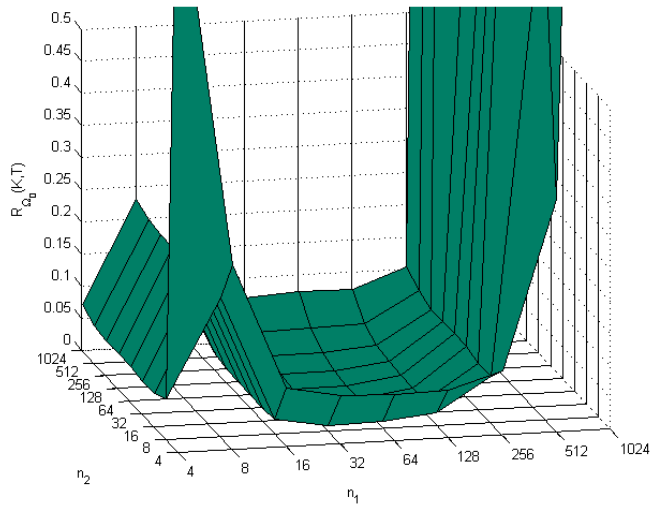

Figure 2: For $\Omega_0 = [0.7, 1.5] \times [0.4, 0.8]$, relative errors $R_{\Omega_0}(K, T)$ for different grid sizes (n_1, n_2) and a noise level $\delta = 10^{-2}$

δ	$n_{1,opt}$	$n_{2,opt}$	$\mathbf{R_{\Omega_0}(K,T)}$
1	16	8	**0.0403**
10^{-2}	32	16	**0.0026**
10^{-4}	64	32	**2.0874e-4**

Table 1: Optimal grid size $(n_{1,opt}, n_{2,opt})$ for Ω_0 when applying the five-point-stencil for $\Omega_0 = [0.7, 1.5] \times [0.4, 0.8]$

required for finite difference differentiators as the error level in the data increases. Herein lies the weakness of traditional finite difference formulas - even if the data are available on a fine grid it cannot be fully utilized. Alternative methods are necessary to recover volatility for the remaining data.

Our numerical experiments show that the approximation of the volatility improves (see table 2) as the strike value K approaches one, which corresponds to "at-the-money" option. This is of special interest since such options are frequently traded. Moreover, in analytic studies of the ill-posedness of the calibration problem for purely time-dependent volatility functions $\sigma^2(T)$, "at-the-money" corresponds to certain singular and extremal situations (see [13, 14, 15]). Furthermore, instability effects are stronger for small maturities T for in-the-money ($K < S$) and out-of-the-money options ($K > S$). Table 2 confirms that the finite difference approach yields good estimates to the volatility close to the "at-the-money" state, and can be used to determine the volatility surface close to $K = 1$. The drawback of this approach is that the volatility can be determined rather stable only in the region of the "at-the-money" state. This is implicit in the structure of

equation (4) because the first derivative with respect to K is multiplied by K whereas the second derivative (in the denominator) is multiplied by K^2. The effect of moving K from $K = 1$ is accentuated by the fact that the first derivative term is in the numerator while the second derivative term is in the denominator.

K^*	$\sigma_e^2(K^*, T^*)$	$\sigma^2(K^*, T^*)$	$R(K^*, T^*)$
0.28	15.07578	0.15990	93.2826
0.61	0.17741	0.17513	0.0130
0.89	0.21392	0.21430	1.7732e-3
0.98	**0.17971**	**0.17973**	**1.1128e-4**
1.03	**0.15719**	**0.15710**	**5.7288e-4**
1.22	0.09433	0.09422	1.1675e-3
1.5	0.15349	0.14966	0.0256
1.82	-0.41689	0.18055	3.3090
2.11	-0.00801	0.15649	0.9488

Table 2: Estimated $\sigma_e^2(K^*, T^*)$ and predefined volatilities $\sigma^2(K^*, T^*)$ for various strikes K^* at $T^* = 0.25$ for the noise level $\delta = 10^{-2}$ on the template $G_0(64, 32)$.

For the noise level $\delta = 10^{-2}$ and different grid sizes (n_1, n_2), relative errors $R(K^*, T^*)$ are shown in figure 3 for two special points, $(K^{*,1}, T^{*,1}) = (0.9, 0.4)$ and $(K^{*,2}, T^{*,2}) = (2, 0.8)$, which are away from the "at-the-money" state. The relative errors for $(K^{*,1}, T^{*,1}) = (0.9, 0.4)$, which is near the "at-the-money" state, have a small variability for different grid sizes (n_1, n_2). Only small and large n_2 cause large relative errors. The variability of the relative errors $(K^{*,2}, T^{*,2}) = (2, 0.8)$, which is far from the "at-the-money" state, are larger. Little changes in (n_1, n_2) cause very different relative errors. This sensitivity does not occur for $(K^{*,1}, T^{*,1})$. This confirms that finite difference schemes yield good approximations to the volatility for the "at-the-money" state $K = 1$. The pattern of the relative errors for different grid sizes, seen in figure 2 for the estimation of the volatility in the region $\Omega_0 = [0.7, 1.5] \times [0.4, 0.8]$, can be observed again in figure 3 where it is more obvious for $(K^{*,1}, T^{*,1}) = (0.9, 0.4)$ than for $(K^{*,2}, T^{*,2}) = (2, 0.8)$.
However, the general aim is to estimate the volatility surface for different K and not only "at-the-money". This yields motivation for the formulation and analysis of an alternative approach.

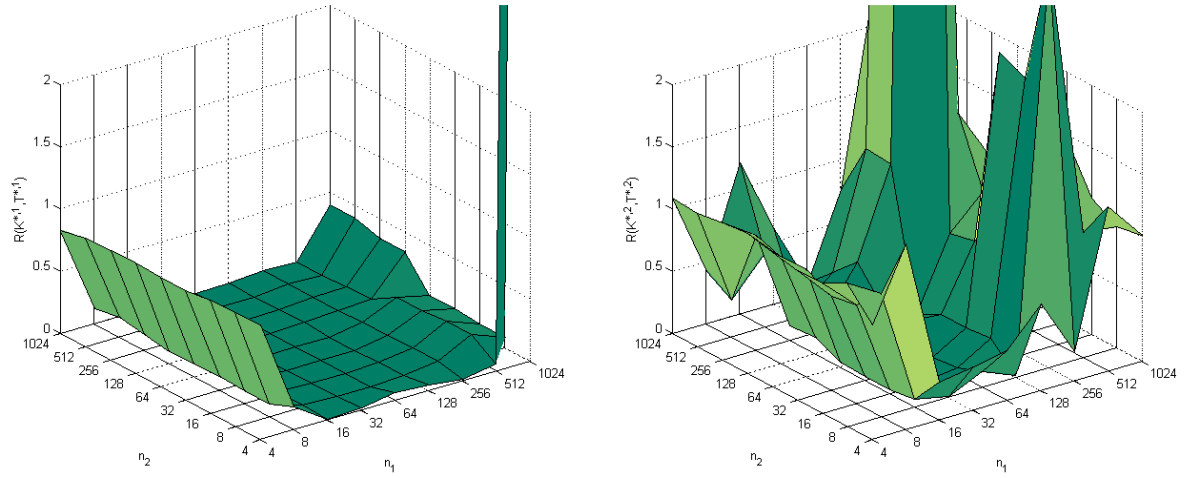

(a) $(K^{*,1}, T^{*,1}) = (0.9, 0.4)$ (b) $(K^{*,2}, T^{*,2}) = (2, 0.8)$

Figure 3: Relative errors $R(K^*, T^*)$ for different grid sizes (n_1, n_2) when applying the finite difference scheme for different points $(K^{*,i}, T^{*,i})$, $i = 1, 2$, with a noise level $\delta = 10^{-2}$

4 Parameter Identification Localization (PILO)

The following alternative approach, based on the ideas of [5], consists of the following four steps (cf. [4]):

1. the weak formulation of Dupire's equation (3),
2. the application of integration by parts to transfer the differentiation of the discrete option prices to the differentiation of the analytic weight function,
3. the localization to a subregion on which the volatility function is assumed to be a constant multiplied by a known shape function which models the local shape of the volatility surface,
4. the choice of the weight function and the local shape.

The application of these steps leads to a constant volatility σ_0^2 on subregion Ω_0. The weak formulation of Dupire's equation (3) is

$$\frac{1}{2}\int_{\Omega} \sigma^2(K,T)K^2 C_{KK}(K,T)w(K,T)dKdT = \int_{\Omega} (C_T(K,T) + rKC_K(K,T))w(K,T)dKdT$$

where we take $\Omega = (0,\, 3S(0)] \times (0, \bar{T}]$ with $S(0)$ being the initial price of the underlying asset, $\bar{T}$ the largest available maturity date and $w(K,T)$ a suitably chosen analytic and

sufficiently smooth weight function. The weight function $w(K,T)$ is localized to some subregion $\Omega_0 \subset \Omega$ with the following properties

$$\begin{aligned} & w(K,T) > 0 \quad \text{in} \quad \Omega_0 \subset \Omega, \qquad\qquad w(K,T) = 0 \quad \text{in} \quad \Omega \backslash \Omega_0 \\ \text{and} \quad & w(K,T) = 0 \quad \text{on} \quad \partial\Omega_0 \end{aligned}$$

and, in addition,

$$w_K(K,T) = w_{KK}(K,T) = w_T(K,T) = 0 \quad \text{on} \quad \partial\Omega_0.$$

The subregion Ω_0 is chosen to be sufficiently small so that

$$\sigma^2(K,T) \approx \sigma_0^2\, \varphi(K,T), \qquad \sigma_0^2 = \text{constant},\ \varphi(K,T) \text{ known on } \Omega_0,$$

is guaranteed. Then the weak formulation above can be rewritten as

$$\frac{\sigma_0^2}{2} \int\limits_{\Omega_0} \varphi(K,T)\, K^2 C_{KK}(K,T) w(K,T) dK dT = \int\limits_{\Omega_0} (C_T(K,T) + rKC_K(K,T)) w(K,T) dK dT \tag{6}$$

Applying integration by parts to equation (6) yields

$$\sigma_0^2 = -2 \ \frac{\int\limits_{\Omega_0} C(K,T) w_T(K,T) + rC(K,T)(Kw(K,T))_K dK dT}{\int\limits_{\Omega_0} C(K,T)(\varphi(K,T)\, K^2 w(K,T))_{KK} dK dT}. \tag{7}$$

As explained in section 2.2, the subregion Ω_0, centered at a chosen (K^*, T^*), is given by $[K_0, K_{n_1}] \times [T_0, T_{n_2}] \subset \Omega$. We use a separable weight function $w(K,T)$, i.e. $w(K,T) = w^{(1)}(T) w^{(2)}(K)$ with

$$\begin{aligned} w^{(1)}(T) &= \begin{cases} (T - T_0)^2 (T - T_{n_2})^2 & \text{if } T \in [T_0, T_{n_2}], \\ 0 & \text{elsewhere}, \end{cases} \\ w^{(2)}(K) &= \begin{cases} -(K - K_0)^3 (K - K_{n_1})^3 & \text{if } K \in [K_0, K_{n_1}], \\ 0 & \text{elsewhere}. \end{cases} \end{aligned} \tag{8}$$

In the sequel, it is assumed that $\varphi(K,T) \equiv 1$.

5 Numerical Performance of the PILO

The purpose of this section is to test the numerical performance of the PILO for the evaluation of the volatility in the neighborhood of a specific location. This then tests the essence of the algorithm - estimate a local constant approximation to the volatility surface. The synthetic option prices, discussed in section 2.1, are used. The basic strategy adopted for achieving this consists of the steps in section 2.2. The evaluation of the integrals in (7) was performed using Simpson's rule.
Initially, let $(K^*, T^*) = (1, 0.5)$, which corresponds to an at-the-money situation. It is of some interest whether the most stable situation is here again associated with $K = 1$. In order to check this, both in-the-money and out-of-the-money scenarios are examined. The region Ω_0 as well as the template $G_0(n_1, n_2)$ are chosen as in section 2.2. For various choices (K^*, T^*), optimal grid sizes (n_1, n_2) are sought that the relative error $R(K^*T^*)$ is minimal. The distance between two grid points are chosen as ΔK^0 and ΔT^0, respectively. To investigate if the assumption of a constant volatility in region Ω_0 is useful, we consider the variability of the volatilities $\sigma^2(K, T)$ in the region Ω_0. This variability can be calculated as the quotient $s_{\sigma^2}/\sigma(K^*, T^*)$ where s_{σ^2} is the standard deviation of the volatilities about $\sigma(K^*, T^*)$. If this variability is small, then it can be assumed with some confidence that $\sigma_e(K^*, T^*)$ has the potential to be representative of the value of the volatility in the Ω_0 neighborhood of (K^*, T^*). For at-the money options, the optimal grid size (n_1, n_2) within Ω_0 for each noise level δ is presented in table 3.

δ	$n_{1,opt}$	$n_{2,opt}$	$R(K^*, T^*)$	$\frac{s_{\sigma^2}}{\sigma^2(K^*,T^*)}$	$\sigma_e^2(K^*, T^*)$
1	62	510	3.9217e-4	0.1291	0.114955
10^{-2}	62	14	4.8780e-4	0.0321	0.115056
10^{-4}	62	14	1.8856e-4	0.0321	0.115022

Table 3: Relative error, the variability of the volatilities and the estimated volatility on Ω_0 for grid sizes $(n_{1,opt}, n_{2,opt})$ at the fixed point $(K^*, T^*) = (1, 0.5)$ with the predetermined synthetic volatility $\sigma^2(K^*, T^*) = 0.115$

At the point $(K^*, T^*) = (1, 0.5)$, the relative error between the estimated and the predetermined volatility function is small so that the localization algorithm can be applied at this point. The described variability of the precise volatility are shown in the fifth column. The variability of the volatilities in Ω_0 for the optimal size is about 3%, except for $\delta = 1$, so that the assumption of an approximately constant volatility in Ω_0 is confirmed. Figure 4 illustrates the variability of the predetermined volatility (green) that is used to obtain the synthetic option prices and the estimated (blue) volatility for a noise level $\delta = 10^{-2}$ and optimal grid sizes $(n_{1,opt}, n_{2,opt}) = (62, 14)$. The distance between the maximal volatility and the minimal volatility amounts 0.0097. Because this is rather small, it can be assumed that the volatility is in the region $\Omega_0 = [1.4773, 1.5227] \times [0.4983, 0.5017]$ constant.

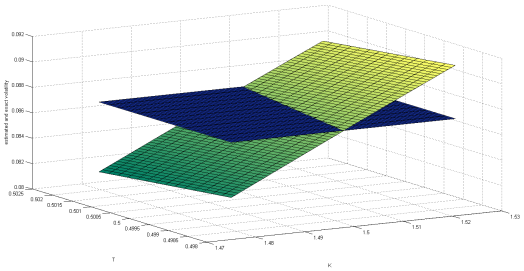

Figure 4: Exact (green) and estimated (blue) volatility for grid size $(n_1, n_2) = (62, 14)$ and noise level $\delta = 10^{-2}$ for point $(K^*, T^*) = (1, 0.5)$

In addition, the sizes of the relative errors at $(K^*, T^*) = (1, 0.5)$ in the fourth column confirm that the localization algorithm yields reliable results. The last column shows the estimated volatility at $(K^*, T^*) = (1, 0.5)$ at which the precise volatility is $\sigma^2(K^*, T^*) = 0.115$. This establishes that the approximation of the volatility at this point by the localization approach is robust and reliable, even when a noise level is $\delta = 1$. This results implies that the PILO works well for at-the-money options.

Table 4 addresses the question whether the PILO yields reliable results also for in-the-money $(K < 1)$ and out-of-the money $(K > 1)$ options for fixed maturity $T^* = 0.5$ and a noise level $\delta = 10^{-2}$. The grid sizes (n_1, n_2) as well as the relative errors $R(K^*, T^*)$ are consistent with the results in table 3. The estimated volatility in column five is close to the predetermined volatility in the sixth column so that the PILO algorithm yields reasonable results for these cases of in-the-money and out-of-the money options.

K^*	$n_{1,opt}$	$n_{2,opt}$	$R(K^*, T^*)$	$\sigma_e^2(K^*, T^*)$	$\sigma^2(K^*, T^*)$
0.5	126	126	18.3206e-4	0.099349	0.099168
1	62	14	4.8780e-4	0.115056	0.115000
1.5	126	6	3.7961e-5	0.086622	0.086619

Table 4: Relative error, the estimated and the predetermined volatility for fixed maturity $T^* = 0.5$ and $\delta = 10^{-2}$

A drawback of the method is the large number of grid points (n_1,n_2) required to estimate the volatility at only one specific point. But, nevertheless the PILO yields a good approximation of the volatility for values of K away from $K = 1$.
Figure 5 shows the relative errors $R(K^*, T^*)$ for various (n_1, n_2) for two different points $(K^{*,1}, T^{*,1}) = (0.9, 0.4)$ and $(K^{*,2}, T^{*,2}) = (2, 0.8)$. Numerical experiments showed that the results and graphics are similar for these points. The structure of the relative errors for different grid sizes (n_1, n_2), when using the PILO, is similar to the structure of the relative errors when the finite difference scheme is applied to evaluate the volatility, cf.

figure 3. The advantage of the PILO is that the structure of the relative errors for points away from $K = 1$, the "at-the-money" state, cf. figure 5(b), is not as susceptible to changes of (n_1, n_2) as the application of the finite difference scheme, cf. figure 3(b).
For both methods, we observe an optimal range for (n_1, n_2) in which the relative error is small. The PILO as well as the finite difference scheme yields poor results outside this range.

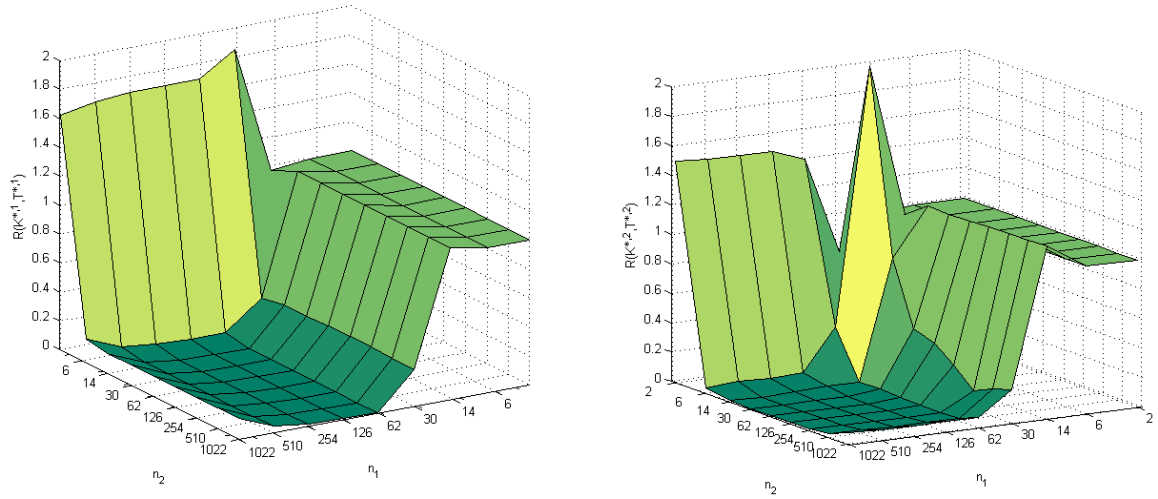

(a) $(K^{*,1}, T^{*,1}) = (0.9, 0.4)$ (b) $(K^{*,2}, T^{*,2}) = (2, 0.8)$

Figure 5: Relative errors $R(K^*, T^*)$ for different grid sizes (n_1, n_2) when applying the PILO for different points $(K^{*,i}, T^{*,i})$, $i = 1, 2$ with a noise level $\delta = 10^{-2}$

6 Conclusions and open questions

Because, for the buying and selling of ECO, it is necessary to determine its fair price, accurate estimates of the volatility $\sigma^2(K, T)$ are required. This leads naturally to the need to explore different numerical methods for its determination. Applying a finite difference scheme to Dupire's formula yields good approximations for "at-the-money" situations. For the finite difference scheme, an optimal range of grid sizes can be observed for points not far from the "at-the-money" state. But, the farther the strike prize K is away from the "at-the-money" state, the less-reliable is the estimate of the volatility. The drawback of this method is that the volatility can be determined rather stable only in the region of at-the-money state.This yielded motivation to consider the identification of the volatility surface from Dupire's equation (3) using its weak formulation. By localizing the problem to a subregion Ω_0 where the volatility function is approximately constant, a new approach is analyzed using representative synthetic data. For a fixed region Ω_0 where σ^2 is essentially constant, the PILO yields good estimates of the volatility. If region Ω_0 is too small,

the estimation of the volatility with the PILO yields no useful results. On the other hand, if Ω_0 is too large, the assumption of a constant volatility in Ω_0 will not be appropriate.
The advantage of the new approach is that the numerical differentiation is replaced by an analytic differentiation of the chosen weight function. In situations where the observational data is sparse, the new method gives a good estimate when applied to representative synthetic data. In particular, the total amount of computational effort required for the implementation of the method is smaller than in case of using regularization approaches. This is a substantial advantage from a practical perspective. An optimal range in which the relative error is small, can be observed not only for points near the "at-the-money" state but also far away.
A drawback of the PILO is the large number of grid points required to estimate the volatility at only one specific point. But drawbacks of the new method can be overcome by applying regularization methods, e.g. Tikhonov regularization [8, 9, 13, 14], to the parameter identification problem of the dual Black-Scholes equation where even convergence rates results are available. However, the total amount of computation required is then much bigger. In our experiments, the function $w(K,T)$ was chosen to be (8). Other choices of $w(K,T)$ may improve the results of the PILO. To evaluate advantages of the new approach further, one could estimate (6) with a function $\varphi(K,T)$ representing a "smile".

Acknowledgement

The second author wishes to acknowledge the support of Johann Radon Institute for Computational and Applied Mathematics (RICAM), Linz/Austria. which fostered and supported the opportunity to commerce and pursue this research collaboration. The third author war supported by Deutsche Forschungsgemeinschaft (DFG) under Grant HO1454/7-2.

References

[1] H.B. Ameur, G. Chavent, and J. Jaffré. Refinement and coarsening indicators for adaptive parametrization: application to the estimation of hydraulic transmissivities. *Inverse Problems*, 18(3):775–794, 2002.

[2] R.S. Anderssen, F. de Hoog, and M. Hegland. A stable finite difference ansatz for higher order differentiation of non-exact data. *Bulletin of the Australian Mathematical Society*, 58:223–232, 1996.

[3] R.S. Anderssen and M. Hegland. For numerical differentiation, dimensionality can be a blessing! *Mathematics of computation*, 68(227):1121–1141, 1999.

[4] R.S. Anderssen and B.P. Lamichhane. Piecewise constant aquifer parameter identification recovery. In *MODSIM2011, 19th International Congress of Modelling and Simulation*, pages 364–370. Modelling and Simulation Society of Australian and New Zealand, 2011.

[5] S.S. Chow and R.S. Anderssen. Determination of the transmissivity zonation using a linear functional strategy. *Inverse Problems*, 7:841–851, 1991.

[6] B. Dupire, editor. *Pricing and hedging with Smiles*, Proceedings of AFFI Conference, La Baule, June 1993.

[7] B. Dupire. Pricing with a Smile. *RISK 7*, pages 14–20, 1994.

[8] H. Egger and H.W. Engl. Tikhonov Regularization Applied to the Inverse Problem of Option Pricing: Convergence Analysis and Rates. *Inverse Problems*, 21:1027–1045, 2005.

[9] H. Egger, T. Hein, and B. Hofmann. On decoupling of volatility smile and term structure in inverse option pricing. *Inverse Problems*, 22:1247–1259, 2006.

[10] M.J. Eppstein and D.E. Dougherty. Simultaneous estimation of transmissivity values and zonation. *Water Resources Research*, 32(11):3321–3336, 1996.

[11] M. Hanke and E. Rösler. Computation of Local Volatilities from Regularized Dupire Equations. *Int. J. Theor. Appl. Finance*, 8(2):207–221, 2005.

[12] M. Hanke and O. Scherzer. Inverse problems light: Numerical differentiation. *Amer. Math. Monthly*, 108(6):512–521, 2001.

[13] T. Hein and B. Hofmann. On the nature of ill-posedness of an inverse problem arising in option pricing. *Inverse Problems*, 19:1319–1338, 2003.

[14] B. Hofmann, B. Kaltenbacher, C. Pöschl, and O. Scherzer. A convergence rates result for Tikhonov regularization in Banach spaces with non-smooth operators. *Inverse Problems*, 23:987–1010, 2007.

[15] B. Hofmann and R. Krämer. On maximum entropy regularization for a specific inverse problem of option pricing. *J. Inverse Ill-Posed Problems*, 13(1):41–63, 2005.

[16] J.C. Hull. *Options, Futures & other Derivatives*. Prentice Hall, 2000.

[17] S. Lu and S.V. Pereverzev. Numerical differentiation from a viewpoint of regularization theory. *Math. Comp.*, 2006.

[18] A. Sepp. Pricing Barrier Options under Local Volatility. *Math. Comp.*, 2002.

[19] P. Wilmott. *Quantitative finance*. Number 1-3. John Wiley & Sons, 2008.

[20] P. Wilmott, J. Dewynne, and S. Howison. *Option pricing: Mathematical models and computation*. Oxford Financial Press, 1995.